Including Croplands in a Global Biosphere Model: Methodology and Evaluation at Specific Sites

Sébastien Gervois, Nathalie de Noblet-Ducoudré,* Nicolas Viovy, and Philippe Ciais

Laboratoire des Sciences du Climat et de l'Environnement, Gif-sur-Yvette, France

Nadine Brisson and Bernard Seguin

INRA, Unité Climat, Sol et Environnement, Avignon, France

Alain Perrier

INAPG, Département AGER, Paris, France

ABSTRACT: There is a strong international demand for quantitative estimates of both carbon sources/sinks, and water availability at the land surface at various spatial scales (regional to global). These estimates can be derived (and usually are) from global biosphere models, which simulate physiological, biogeochemical, and biophysical processes, using a variety of plant functional types. Now, the representation of the large area covered with managed land (e.g., croplands, grasslands) is still rather basic in these models, which were first designed to simulate natural ecosystems, while more and more

_____

* Corresponding author address: Nathalie de Noblet-Ducoudré, Laboratoire des Sciences du Climat et de l'Environnement Unité mixte CEA-CNRS, Bât 701 Orme des Merisiers, 91191 Gif-sur-Yvette cédex, France.

E-mail address: Nathalie.De-Noblet@cea.fr

land is heavily disturbed by man (crops cover ~35% and grasslands ~30%–40% of western Europe's area as a result of massive deforestation mainly in the Middle Ages).

In this paper a methodology is presented that combines the use of a dynamic global vegetation model (DGVM) known as Organizing Carbon and Hydrology in Dynamic Ecosystems (ORCHIDEE) and a generic crop model [the Simulateur Multidisciplinaire pour les Cultures Standard (STICS)]. This association aims at improving the simulation of water vapor and CO_2 fluxes at the land–atmosphere interface over croplands, and thereby the calculation of the carbon and water budget. Variables that are much better computed in STICS (e.g., leaf area index, root density profile, nitrogen stress, vegetation height) are assimilated daily into ORCHIDEE, which continues to compute its own carbon and water balance from the fluxes simulated at the half-hourly time step. The allocation of photosynthates in ORCHIDEE was modified in order to maintain the coherence between leaf area index and leaf biomass, as well as between root density and root biomass. Soil moisture stress is computed using a more realistic root density profile. The maximum rates of carboxylation and RuBP (ribulosebisphosphate) regeneration were adjusted to more realistic values, while the actual rates can now be reduced following the nitrogen stress. Finally, harvest has been implemented into ORCHIDEE.

The improved model (ORCHIDEE-STICS) is evaluated against measurements of total aboveground biomass, evapotranspiration, and net CO_2 flux at four different sites covered with either winter wheat or corn.

KEYWORDS: Global biosphere model; Ecosystems: managed and natural; Water, carbon, and energy budget

1. Introduction

Human activities have been transforming the natural landscape for thousands of years (Vitousek et al. 1997) and will most probably continue to transform it (Alcamo et al. 1998). This has had, and will have, many impacts, including effects on regional and global climates. Many modeling studies of the interactions between climate and vegetation compared disturbed lands with natural vegetation, mostly in the Tropics where forests were, and are still, being converted into croplands or grasslands (e.g., Nobre et al. 1991; Xue and Shukla 1993; Polcher et al. 1996). These numerical experiments showed large regional impacts on the water cycle, including local inflow of atmospheric water vapor. More recently, modelers focused on the temperate zone. For instance, Betts (Betts 1999) simulated cooler European summers as a result of increased surface albedo, while Zhao et al. (Zhao et al. 2001) obtained warmer summers due to decreased evapotranspiration. Over western Europe, de Noblet-Ducoudré (2005) simulated milder and wetter winters, and cooler summers, caused by both increased albedo and greater evapotranspiration rates when comparing present-day land cover with potential vegetation distribution (e.g., before the large deforestation of the Middle Ages). These modeling studies all agree that land-cover changes can have a significant impact on regional (and possibly global) climates, although their results differ quantitatively, and sometimes qualitatively. Interestingly, in all cases croplands were simply

treated as "modified grasslands" because, up to now, crop models able to represent agroecosystems in a realistic way have only been designed and used for specific predictions and analyses at the site or field level and their integration in global models had not been considered.

Another rather large set of studies, using empirical models, has also shown the potential impacts of croplands on the carbon budget. Apart from the well-known release of carbon dioxide occurring when pristine forests are being replaced by crops, the role of croplands (supply of carbon to or removal from the atmosphere) is yet highly uncertain and depends on the management mode (Smith et al. 2000). Vleeshouwers and Verhagen (Vleeshouwers and Verhagen 2002) showed that European croplands act as a carbon source of about 0.84 TC ha^{-1} yr^{-1} but with very large uncertainties (Janssens et al. 2003). This is in agreement with more and more evidence of lower soil carbon content under cultivated areas than in natural ecosystems (Arrouays et al. 2002).

At the global scale, we know from more recent studies (Dufresne et al. 2002; Friedlingstein et al. 2003; Cox et al. 2000) that land surfaces may not be able to absorb in the next century as much CO_2 as they do now due to the expected warming and therefore may not compensate much for the future increase in anthropogenic emissions of carbon dioxide. These pioneer experiments have not considered a potential changing landscape, neither have they included a realistic representation of present-day functioning of croplands, which may even exacerbate the negative feedbacks they have highlighted.

All these considerations, together with the known poor representation of crops and pastures in most biogeochemical and soil–vegetation–atmosphere transfer global models, justify any work trying to improve the description of these ecosystems in global biosphere models.

Global biosphere models encapsulate natural biogeochemical and biophysical processes in order to simulate important ecosystems processes (e.g., photosynthesis, respiration, and allocation) at a large spatial scale, and are often designed to be coupled with atmospheric general circulation models. Such global spatially explicit models generally have only few plant functional types, and they treat croplands in a crude manner. Because land managers strictly control the development of plants in agroecosystems by means of fertilization and irrigation calendars, and choice of sowing date, the ecosystem can no longer be treated as being governed only by natural processes.

Crops, being the major source of food and fibers, have been studied for a long time in order to increase yield (e.g., du Monceau 1761), and agronomists have designed and applied plant growth models over the last 30 yr for that purpose (de Wit 1978; Ritchie and Omer 1984; Jones and Kiniry 1986). There are as many models as crop types, each generally having been calibrated for one crop family only. However, generic crop models have recently been developed: DAISY (Danish Simulation Model; Hansen et al. 1990), the Explicit Planetary Isentropic Coordinate model (EPIC; Williams et al. 1984), the World Food Study model (WOFOST; van Deipen et al. 1989), and the Simulateur Multidisciplinaire pour les Cultures Standard (STICS; Brisson et al. 1998).

In this paper we focus on one global ecosystem model [Organizing Carbon and

Hydrology in Dynamic Ecosystems (ORCHIDEE)] and one crop model (STICS). ORCHIDEE has been developed by Krinner et al. (2005), is coupled to the Institut Pierre Simon Laplace (IPSL)[1] atmosphere–ocean general circulation model (http://www.ipsl.jussieu.fr/~omamce/IPSLCM4) and will be further used in studies estimating the changes in 1) global carbon sources/sinks and 2) climate due to human-induced changes in land cover. STICS (Brisson et al. 1998) simulates the growth of several temperate crop types (e.g., wheat, corn, and soybean) and is also being extended to tropical crops (e.g., bananas) that may be important for the potential use of the model in global studies.

Our objective is to improve the simulation of fluxes by ORCHIDEE at the surface–atmosphere interface over croplands and to allow further studies of the simultaneous interactions between climate, land management, and crop growth. Section 2 shows why natural grass plant functional types (PFTs) cannot be used, in global ecosystem models, as a substitute for crops. Section 3 describes the models and the methodology chosen for "coupling." Section 4 shows results of our coupled model at a number of specific sites covered with either winter wheat or corn. Conclusions are drawn in section 5.

2. Why crops cannot be further simulated in a DGVM with natural grass PFTs as a substitution

Until now, crops are parameterized as natural grasslands in global ecosystem models (as in ORCHIDEE), albeit with modifications of some parameters. Examination of the simulated leaf area index (LAI; i.e., leaf surface area per unit ground surface area) is a good way to evaluate the first-order response of the model since LAI is a key variable that impacts the following:

- albedo,
- roughness length,
- penetration of radiation in the canopy,
- canopy conductance,

and thereby most surface fluxes (e.g., radiation, latent and sensible heat, and photosynthesis).

In its standard version (see section 3.1.) ORCHIDEE uses natural grasslands as a substitute for crops and Figure 1 compares its simulated LAI with 1) the observed and 2) the LAI simulated by the crop model STICS (described in section 3.2.), at two different sites (Table 1): a winter wheat site located near the Institut National de Recherche Agronomique (INRA) center in Grignon, France, and a corn site located in Poitou-Charentes, France.

It is rather obvious that ORCHIDEE is unable to correctly simulate the seasonality of a winter crop (Figure 1a), while STICS's outputs match very well with the observed data. Winter wheat is usually sown in France in October–November, emerges before winter, and reaches its maximum LAI in the spring before being harvested in early summer. In ORCHIDEE, wheat is modeled as a

---

[1] The IPSL is a federation of research laboratories and universities that are located in and close to Paris, France (headed by Jean Jouzel).
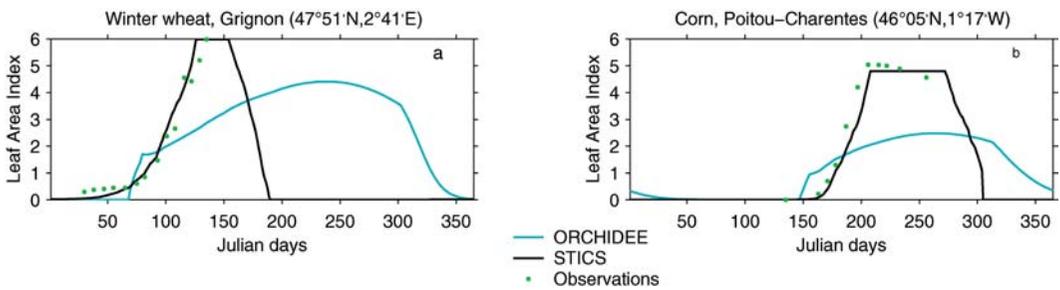
Figure 1. Observed discrepancy between ORCHIDEE vs STICS and data. Temporal evolution of observed (green triangles) and simulated (plain lines) LAI starting 1 Jan (Julian day 1) and ending 31 Dec (Julian day 365). Simulated values from STICS are plotted using the black line, while results from the standard version of ORCHIDEE are plotted using the blue line. Results are shown for (a) winter wheat at Grignon in 1995, and (b) corn in Poitou-Charentes in 1996. Both sites are briefly described in Table 1.

natural C_3 grass (albeit with enhanced photosynthesis), hence, its growth curve more closely follows the climatic conditions as germination occurs in the spring and a maximum LAI is reached in late summer. The timing problem is not as crucial for corn (Figure 1b) as this cereal is sown in the spring and therefore emerges at the same time as a natural grass.

Moreover, not only is the maximum value of the simulated LAI greatly underestimated by ORCHIDEE, but also the simulated growing season is too long in ORCHIDEE at both sites.

Most of these differences are due to anthropogenic processes that are accounted for in STICS (implicitly or explicitly) but not in ORCHIDEE:

Table 1. Some characteristics of each of the four sites used in this paper for evaluation of ORCHIDEE-STICS. For LAI, biomass, evaporation, and carbon flux, the "yes" indicates that we had access to measurements, while "no" means no data were available.

Name	Year	Country	Crop type	Annual mean temperature (°C)	Longi-tude	Lati-tude	Alti-tude	LAI	Bio-mass	Evapo-transpir-ation	Net carbon flux
Grigon	1995	France	Winter wheat	10	47°51′N	02°41′E	120 m	Yes	Yes	No	No
Poitou-Charentes	1996	France	Corn	11.5	46°05′N	01°17′W	80 m	Yes	Yes	No	No
Bondville	1997	USA (Illinois)	Corn	11.1	40°00′N	88°17′W	300 m	Yes	No	Yes	Yes
Ponca	1997	USA (Oklahoma)	Winter wheat	16	36°45′N	97°05′W	250 m	No	No	Yes	Yes

- selection of crop cultivars drive high LAI and short seasonal cycles;
- agricultural practices applied by farmers (e.g., ploughing; choice of sowing date; frequency, type, and amount of fertilizer; irrigation; and harvest date) modulate the timing and duration of the growth cycle and crop growth amplitude.

3. Models and "coupling" strategy

The quick overview of the main processes simulated in each model, presented in sections 3.1. and 3.2., is followed by the detailed methodology adopted to "couple" both models.

3.1. ORCHIDEE

ORCHIDEE (Krinner et al. 2005; Figure 2, upper part) is the land surface model ("carbon–water–energy") developed at IPSL. It simulates water, CO_2, and energy exchanges between vegetation and the atmosphere and can be used either coupled to the IPSL climate model or offline as it was in this study (i.e., forced with observed meteorological data). Its time step for a number of processes is 30 min, ensuring numerical stability and adequate representation of the diurnal cycle. ORCHIDEE includes three main modules.

- The Soil–Vegetation–Atmosphere Transfer Scheme [Schématisation des Echanges Hydriques à l'Interface entre le Biosphère et l'Atmosphère (SECHIBA; Ducoudré et al. 1993], which interacts with the atmosphere and computes the "instantaneous" (fast, i.e., half-hourly time step) fluxes of momentum, heat, water, and CO_2 assimilation, the soil water budget, and the surface energy budget.
- A biogeochemical model that simulates the daily processes of carbon and vegetation dynamics (e.g., respiration, litter production and decomposition, allocation, leaf cycle).
- A module of long-term (i.e., more than 1 yr) ecosystem dynamics (i.e., evolution from one vegetation type to another), extracted from the Lund–Potsdam–Jena (LPJ) Dynamic Global Vegetation Model (DGVM; Sitch et al. 2003). In this study this module is turned off since the distribution of vegetation was always prescribed.

Surface types are grouped into 10 natural PFTs (e.g., evergreen and deciduous trees, C_4 and C_3 grass) and bare soil. Two additional PFTs, abusively named crops (C_3 and C_4), are included, but in reality they correspond to a "supergrassland" (the only differences with natural C_3 and C_4 grass PFTs are the prescribed higher rates of carboxylation and RuBP (ribulosebisphosphate) regeneration, so as to simulate greater productivity). PFTs can coexist within the same cell (also referred to as a mosaic vegetation). They all experience the same climate forcing but compute fluxes depending on their own properties. The fluxes are thereafter averaged before entering the first atmospheric level.

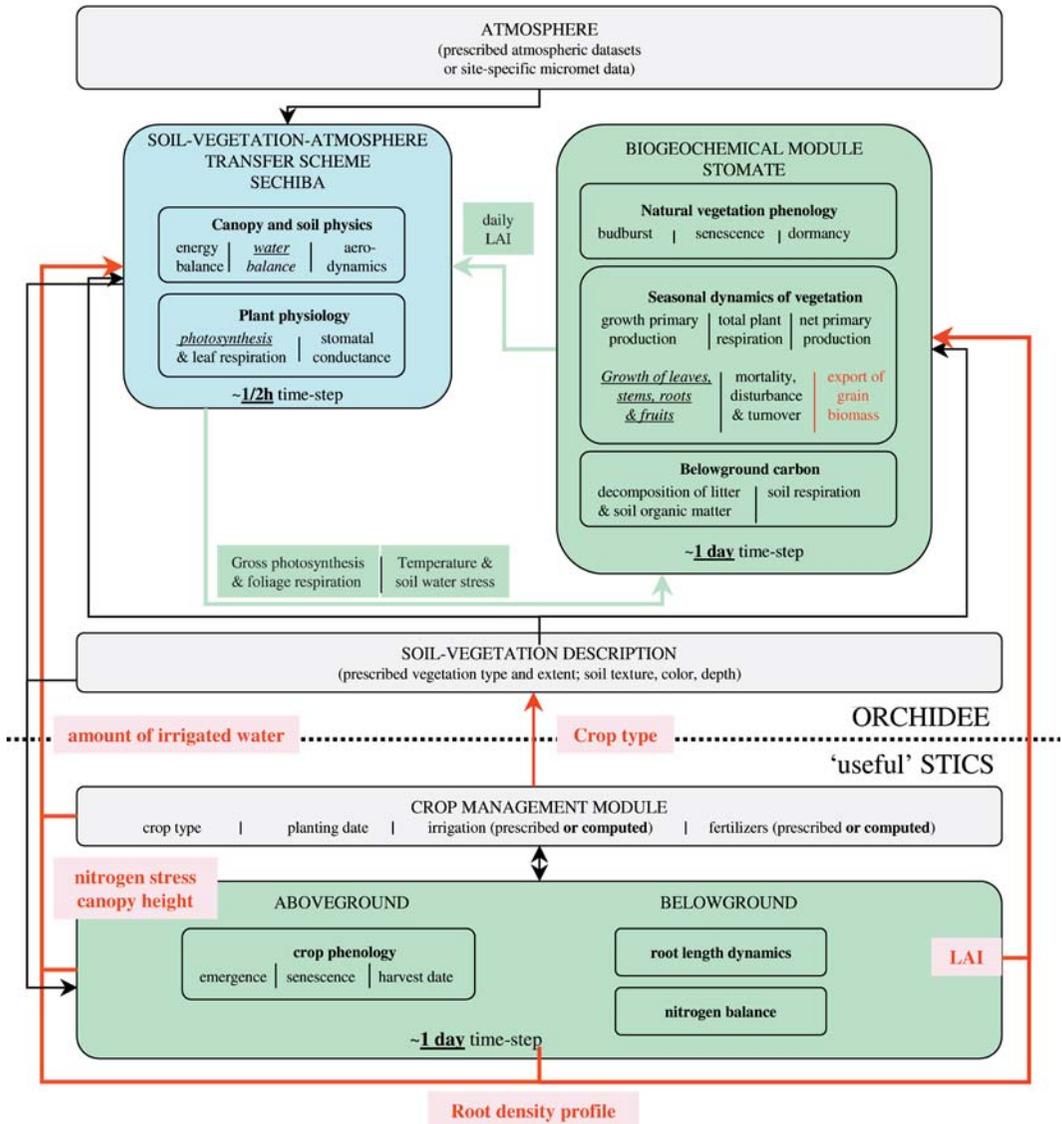## ORCHIDEE-STICS Structure

Figure 2. Schematic of ORCHIDEE-STICS, an altered version of ORCHIDEE (Krinner et al. 2005), ORCHIDEE-STICS incorporates agroecosystems using crop phenology, crop management (e.g., fertilizer application, irrigation), and nitrogen cycling. Red arrows and text indicate the variables that are simulated by STICS and assimilated in ORCHIDEE. Text in italics and underlined indicates parameterizations of ORCHIDEE that have been updated. Blue boxes refer to fast processes (time step smaller than 1 h), while green boxes refer to processes/variables computed daily. Gray boxes show prescribed variables.

3.2. STICS

STICS[2] (Brisson et al. 1998; Brisson et al. 2002a; Brisson et al. 2002b) has been developed and extensively validated as an operational tool to compute crop yield and quality, as well as environmental variables. It simulates the daily behavior of the soil–crop system (e.g., aboveground biomass and its nitrogen content, leaf area index, number of harvested grains and their biomass, soil water and nitrogen budgets, and root density profile). STICS has been applied to a variety of crops and cultivars (e.g., wheat, corn, tomato, banana, soybean, grass, and grape) with few structural changes. Some calculating modes, parameters, and management prescriptions (e.g., sowing date, amount of fertilizers, amount of irrigation) are specific to the chosen crop type (or cultivar).

STICS is divided into several modules concerning the aboveground part of the crop (i.e., leaf area index and biomass, and allocation to grains), soil water and nitrogen balance, root growth, and the transfer of water and nutrients between the soil and the aboveground biomass through the roots.

3.3. Assimilating outputs from STICS in ORCHIDEE

As already highlighted in section 2, STICS realistically simulates the "real crop world" despite a limited use of mechanistic modeling (of physiological and biophysical processes common to all crop models as discussed in Boote et al. 1996). Therefore, rather than implementing improved parameterizations for crops in ORCHIDEE, the strategy we have adopted is to assimilate some of STICS's outputs in ORCHIDEE to replace the variables that are either badly simulated (e.g., LAI) or crudely prescribed (e.g., nitrogen stress and vegetation height). This will allow us to implement all useful future improvements of STICS without (or with minimum) further adjustments of ORCHIDEE.

We could have chosen to use STICS instead of ORCHIDEE over cultivated areas, but coupling with climate would not have been possible as we would have lacked short-term exchanges with the atmosphere (e.g., water, heat, momentum, CO_2). Just as important, evaluation of changes in stocks of soil carbon and water at any spatial scale (regional to global) requires that these budgets be coherently simulated. This can only be done using the same modeling approach. Differences that can arise from the use of different models can indeed be as large as the ones resulting from missing feedbacks in only one model.

Each model is run simultaneously and forced with the same atmospheric conditions and surface characteristics (see Figure 2 for schematic diagram). Each day, STICS provides ORCHIDEE with values for LAI, root density profile, nitrogen stress, and vegetation height. Some parameterizations had to be updated in ORCHIDEE: 1) the computation of carbon allocation to plant compartments and leaf senescence was changed to ensure consistency between the LAI (root density profile, respectively) from STICS and the leaf biomass (root biomass, respectively) computed in ORCHIDEE (see section 3.3.); and 2) the soil moisture stress to account for the root density profile computed in STICS (see section 3.4.).

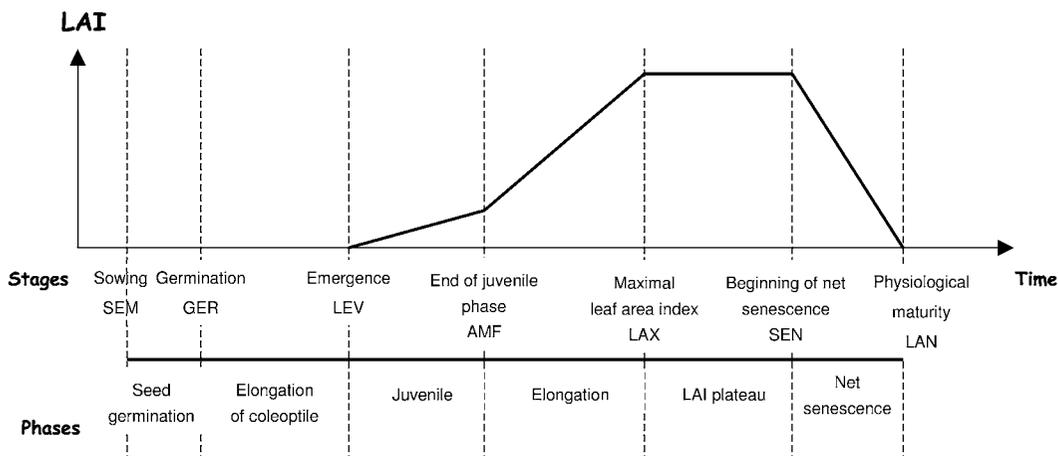[2] In this study we have used version 4.0 of STICS.

Figure 3. Theoretical temporal evolution of LAI in STICS.

3.3.1. Seasonal cycle of leaf area index

The temporal evolution of LAI in STICS is composed of several phases after crop emergence (Figure 3): the juvenile phase, the elongation phase (period of maximum growth), a plateau of maximum LAI (during which growth and senescence compensate for each other), and finally loss of all foliage as the rate of senescence outweighs any growth. The duration of each phase is calculated from growing degree-day sum (GDD; based on crop temperature above prescribed base temperature) weighted by limiting functions to account for photoperiodism (e.g., for wheat and soybean), and vernalization (e.g., for winter wheat). Transition between stages occurs at prescribed values of GDD sums, which are specific to each crop and cultivar (see values in Table 2 for winter wheat and corn).

Emergence depends on the number of GDDs accumulated since the sowing date computed using soil temperature at the sowing depth. Emergence will not occur if soil moisture in the seed-bed layer is below the wilting point.

LAI is, up to maturity, computed as the net balance between leaf growth and senescence. Daily growth is a logistic function of development units (corresponding to the different stages) multiplied by crop efficient temperature and stress

Table 2. Values of GDD sums used for winter wheat and corn at all sites to compute the temporal cycle of LAI (see Figure 3 for nomenclature).

Growth stages/thresholds	Winter wheat GDD above 0°C	Corn GDD above 8°C
Between sowing date and emergence	51	128
Between emergence and the end of the juvenile stage	237	405
Between the end of the juvenile stage and maximun LAI	310	403
Between maximum LAI and the start of senescence	237	744
Between the start of senescence and physiological maturity	693	309
TOTAL	1522	1989

functions related to water and nitrogen limitations. After the maximum growth period, LAI remains constant (at its maximum value) until the beginning of net senescence and is then considered to decrease linearly to zero (Brisson et al. 1998).

In STICS, growth in terms of biomass is computed independently and only influences the leaf growth in terms of surface if the inferred specific leaf area (i.e., the ratio between leaf surface area and leaf dry mass) reaches critical values.

In ORCHIDEE, the date of leaf emergence is computed from Botta et al. (Botta et al. 2000) and depends (as for STICS) on GDD sums and soil water availability. The plant then uses its carbohydrate reserve (accumulated during the previous year and corresponding to seeds for crops) to grow a minimum quantity of leaves and roots. If this carbohydrate reserve is empty, the plant will not be able to grow. Once the growing season has started, photosynthesis and respiration are computed as functions of atmospheric conditions, leaf age, and species characteristics, and photosynthetates are allocated to the different plant compartments following the formulations derived by Friedlingstein et al. (Friedlingstein et al. 1998; see section 3.3.1). LAI is finally computed daily from the amount of biomass allocated to leaves as follows:

$$\text{LAI} = \text{leaf\_biomass} \times \text{sla},$$

where sla is the specific leaf area (m^2 gC^{-1}). A maximum value of LAI is prescribed for each plant type, above which no more biomass is allocated to leaves. Senescence occurs either when leaves reach a prescribed age or when the stress threshold related to temperature or soil water content is met.

Because the LAI displays incorrect seasonality and climax (Figure 1), we have chosen to inhibit its daily calculation in ORCHIDEE and to replace it with the one computed daily in STICS.

3.3.2. Photosynthesis

In ORCHIDEE, C_3 photosynthesis (e.g., winter wheat) is computed from Farquhar et al. (Farquhar et al. 1980), while for C_4 plants (e.g., corn) the model developed by Collatz et al. (Collatz et al. 1992) is used (photorespiration being inhibited in C_4 plants). In both cases, photosynthetic rates depend on maximum rates of carboxylation ($V_{c\max}$) and RuBP regeneration ($V_{j\max}$), which are, respectively, set to 100 and 200 μmol s^{-1} m^{-2} (for a temperature of 25°C) in the standard version of ORCHIDEE for both C_3 and C_4 crops. These parameters were updated in the new version of the code to $V_{c\max} = 120$ and $V_{j\max} = 240$ μmol s^{-1} m^{-2} following the data compilation of Wullschleger (Wullschleger 1993). Higher values (compared to natural grass PFTs) result mainly from the genetic selection of cultivars.

3.3.3. Allocation, senescence, and harvest

We have modified our carbon allocation procedure to reconcile the calculation of leaf biomass with the externally forced LAI. In the standard version of ORCHIDEE this has been adapted from Friedlingstein et al. [Friedlingstein et al. 1998; see Krinner et al. (2005) for further discussion] and accounts for five biomass compartments (leaves, roots, stems, reserves, and fruits). The fractions allocated to leaves, roots, and stems are parameterized as functions of soil water

content, temperature, light, and nitrogen availability (e.g., stress functions). At the end of the growing season all photosynthetates are allocated to the carbohydrate reserves (that will be used for the next season's leaf and root initial growth). Otherwise, the fraction allocated to fruits is set to 10%. As already mentioned (see section 3.3.1.), no more biomass is allocated to leaves above the maximum prescribed LAI.

To improve ORCHIDEE we included a sixth reservoir, "export," that is only filled at harvest with the sum of fruit and reserve biomass (the fruit reservoir is then immediately set to zero, while a minimum biomass is kept in the reserve for the next season's growth). Senescent stems and leaves are converted into locally decomposing litter.

The daily increment in leaf biomass (NPP_l) is computed from the daily increment in LAI ($d\text{LAI}/dt$) simulated by STICS as follows:

$$NPP_l = \frac{d\text{LAI}}{dt} \frac{1}{(\text{sla})}.$$

Similarly, the daily increment in root biomass (NPP_r) in the updated version of ORCHIDEE is computed from the daily increment in root length ($d[\int_0^{z_r} L_r(z)]/dt$; see section 3.3.4.) simulated in STICS:

$$NPP_r = \frac{d\left[\int_0^{z_r} L_r(z)\right]}{dt}\left(\frac{1}{L_{r0}}\right),$$

where L_{r0} is the specific root length set to 18×10^3 cm gC^{-1} for wheat and to 9×10^3 cm gC^{-1} for corn (Gregory et al. 1997); $L_r(z)$ is the root length as a function of depth (z); and z_r is the root front depth simulated in STICS.

The remaining daily net primary production (NPP_{residual}), once NPP_l and NPP_r have been computed, is allocated to the other compartments (i.e., fruits, stems, and reserves), with the same proportionality coefficients as computed in the standard version of ORCHIDEE. If NPP_{residual} is negative (i.e., $NPP_l + NPP_r >$ daily total NPP), nothing can be allocated to fruits and stems, and the required amount is removed from the reserves (i.e., $NPP_l + NPP_r - NPP$). If the extreme case occurs in which the reserves are not sufficient, then the amounts allocated to leaves and roots have to be reduced, while conserving the ratio between them, but the consistencies between LAI and leaf biomass, root length, and root biomass are lost. This extreme case will only happen if the reserves (put aside at last year's harvest) at the sowing date are not sufficient to represent the amount of seeds that have actually been sown.

Leaf net senescence in our updated version of ORCHIDEE starts when the daily increment of LAI becomes negative. Then, the daily amount of dead aboveground biomass (Q_l), which immediately becomes metabolic litter (i.e., sugars and cellulose with fast decomposition), is computed as follows:

$$Q_l = -\frac{d\text{LAI}}{dt}\left(\frac{1}{\text{sla}}\right).$$

Dead roots are similarly added to the belowground metabolic litter.

3.3.4. Root density profile and soil moisture stress

Soil moisture in ORCHIDEE controls transpiration and bare ground evaporation through a water uptake function (U_s). This function is based on the assumption that the vertical root density profile [$R(z)$] is nearly exponential (Ducoudré et al. 1993; de Rosnay and Polcher 1998):

$$R(z) = e^{-cz},$$

where c is a single number per plant type describing the profile set to 4 m^{-1} for all crops.

The soil column in ORCHIDEE consists of two layers (Choisnel 1977). The upper layer is of variable depth and is created when precipitation (P) exceeds evapotranspiration (ETR). When ETR rises over P, the lower reservoir behaves as a bucket model. A step function was chosen to define the moisture profile in each layer with a dry soil height (h_{id} for the ith reservoir) below which the soil is at saturation and above which the soil is dry. For the ith layer U_s is computed as

$$U_{is} = e^{-ch_{id}}.$$

STICS daily computes a root density profile that can be quite different from the one used in ORCHIDEE (Figure 4), with fewer roots in the upper 20 cm of soil and more below. The depth of the root front (Z_r) is an important variable that determines the maximum depth from which plants can extract water (Z_r can be much lower than the maximum soil depth considered at each site, especially at the beginning of the growing season). Here Z_r equals 0 at the sowing depth and
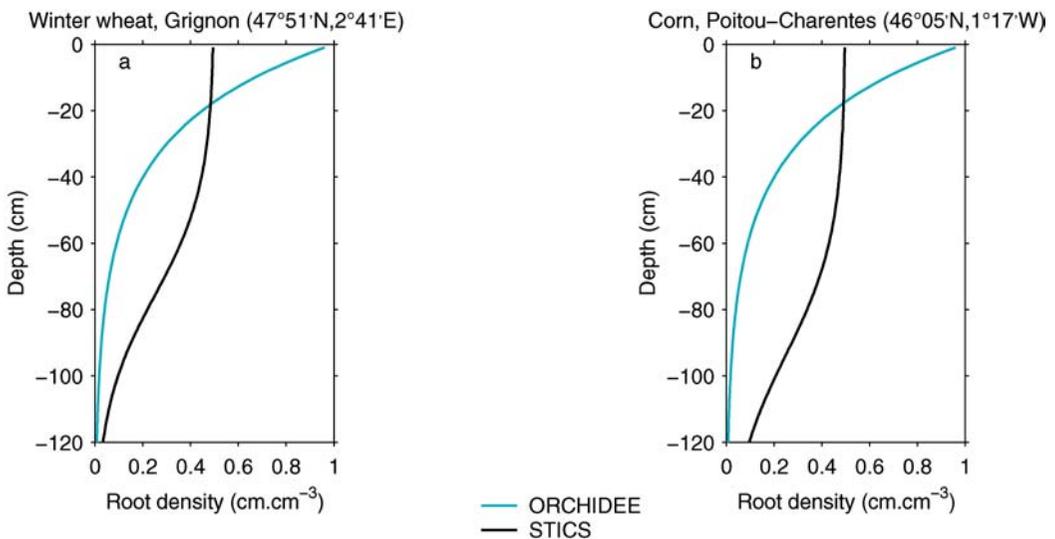

Figure 4. Mean root density profile when LAI has reached its maximum values. Simulated values from STICS are plotted using the black line, while prescribed values for ORCHIDEE are plotted using the blue line. Results are shown for (a) winter wheat at Grignon in 1995 and (b) corn in Poitou-Charentes in 1996.

increases until it reaches the prescribed bottom of the soil, or until LAI reaches its maximum value (see section 3.3.1.) The root length is computed as a function of depth [$L_r(z)$: set to 0 below Z_r)] following formulations similar to the ones used for LAI (i.e., using the GDD concept). When this simulated root density profile is used in ORCHIDEE instead of the original exponential function, U_{is} then becomes

$$U_{is} = \int_{h_{id}}^{h_i} L_r(z)dz \bigg/ \int_0^{h_i} L_r(z)dz,$$

where h_i is the total depth of the ith layer (equal to 0 at ground surface). Relative soil moisture in each layer is therefore simply computed as the ratio between the density of roots that are immersed in water and the total root density in the layer.

3.3.5. Vegetation height

Vegetation height is used together with LAI to compute roughness length and therefore affects all turbulent fluxes (e.g., evapotranspiration and sensible heat flux). It is prescribed in ORCHIDEE for each PFT and does not vary with time. Crops, for example, never exceed 5 cm (as for a natural grass), whereas in reality they are much taller during the growing season (80 cm to 2 m).

STICS, on the other hand, computes a daily crop height that we have decided to use in ORCHIDEE instead of the prescribed value.

Increasing the vegetation height results in increased roughness length and decreased aerodynamic resistance. This has a direct impact on the turbulent heat fluxes and thereby on surface temperature.

3.3.6. Nitrogen stress

ORCHIDEE, in its standard version, is unable to account for nitrogen stress, while even at crop sites, stress can occur if fertilizers are not brought in sufficient quantity.

To more properly account for this, we have multiplied the rates of carboxylation and RuBP regeneration simulated by ORCHIDEE by the nitrogen stress (a function varying between 0 and 1) simulated by STICS. In the following, ORCHIDEE will refer to the standard version of our code, while ORCHIDEE-STICS will refer to the version accounting for the improvements described in this section.

4. Evaluation of ORCHIDEE-STICS at specific sites

ORCHIDEE-STICS simulations were carried out at four different sites where meteorological, site-specific, and validation data were available (Table 1). Total aboveground biomass had only been measured at two sites, evapotranspiration and net CO_2 flux at two other sites. Meteorological data include rainfall, wind speed, incoming solar and infrared radiation, ambient air temperature, and ambient air relative humidity. Where information on irrigation, fertilization, and harvest were not available, STICS was allowed to compute its own calendars and amounts applied. Two of the sites chosen are located in France, while the other two are
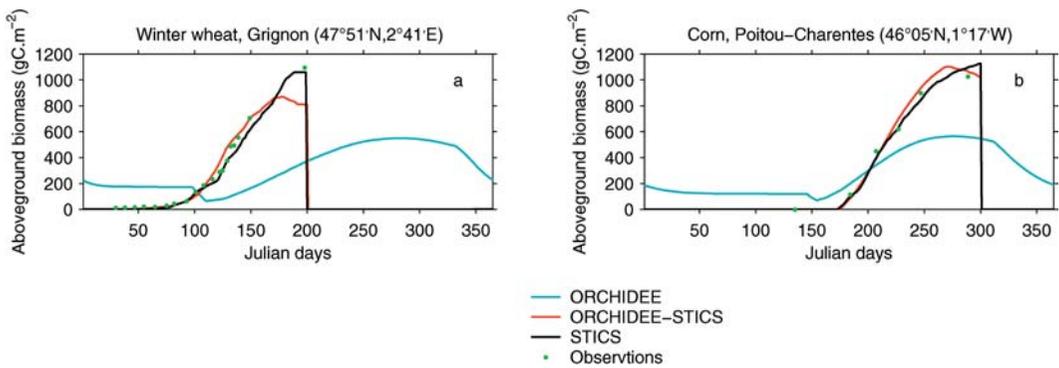
Figure 5. Temporal evolution of observed (green triangles) and simulated (plain lines) total aboveground biomass (gC m^{-2}) starting 1 Jan (Julian day 1) and ending 31 Dec (Julian day 365). Simulated values from STICS are plotted using the black line, results from ORCHIDEE are plotted using the blue line, and those from ORCHIDEE-STICS are plotted using the red line. Results are shown for (a) winter wheat at Grignon in 1995 and (b) corn in Poitou-Charentes in 1996.

located in the United States. The same cultivar choice was made in the model at all sites for winter wheat and for corn (see Table 2). Because the American cultivars are probably not the same as the French, this approximation may lead to some discrepancies between the simulated and observed values, but our assumption here is that the major improvement in the variables and fluxes simulated by ORCHIDEE will be achieved by the changes introduced, rather than by the choice of the exact cultivar (Kucharik 2003).

4.1. Evaluation of total aboveground biomass

Aboveground biomass is the main variable against which crop models are regularly evaluated and is the first one we have chosen for ORCHIDEE-STICS to highlight the benefits of coupling both models. Figure 5 shows, for the two French sites chosen, the observed seasonality of total aboveground biomass, together with the ones simulated by the standard version of ORCHIDEE, by STICS, and by ORCHIDEE-STICS. The largest difference is obtained for winter wheat (see discussion in section 2). At both sites the timing is predicted more accurately by ORCHIDEE-STICS, and the amplitude is increased in response to the larger LAI values.

Aboveground biomass increases in ORCHIDEE-STICS until day 160 for wheat and 265 for corn, and then decreases following the decrease in LAI (Figure 1) and the immediate conversion of senescent leaves into litter (no standing dead biomass in ORCHIDEE-STICS). In STICS, on the other hand (as in reality), the decrease in aboveground biomass does not start before harvest because dead biomass only becomes litter at the last moment. This explains the apparent underestimation of the peak value that is rubbed out if litter is added to standing (and living) biomass in ORCHIDEE-STICS.

The three major changes that have a significant impact at these sites are, in

Table 3. Description of all simulations carried out to evaluate, step by step, the impact of the changes we made to ORCHIDEE. Simulation S6 corresponds to the final version: ORCHIDEE-STICS, while simulation S0 corresponds to the standard ORCHIDEE.

Name	LAI	V_{cmax}	Nitrogen stress	Alocation, senescence and export of grains	Root profile	Vegetation height
S0 ORCHIDEE	Computed	100	–	Standard	Prescribed	Prescribed
S1	From STICS	100	–	Standard	Prescribed	Prescribed
S2	From STICS	120	–	Standard	Prescribed	Prescribed
S3	From STICS	120	–	Modified	Prescribed	Prescribed
S4	From STICS	120	–	Modified	From STICS	Prescribed
S5	From STICS	120	–	Modified	From STICS	From STICS
S6 ORCHIDEE-STICS	From STICS	120	From STICS	Modified	From STICS	From STICS

decreasing order (Tables 3, 4, and 5; Figure 6): 1) the assimilation of LAI values simulated by STICS (section 3.3.1.); 2) the update of the allocation procedure and senescence, and the inclusion of export biomass (section 3.3.3.); and 3) the update of maximum rates of carboxylation and RuBP regeneration from natural grass to crop values (section 3.3.2.). Accounting for the simulated nitrogen stress becomes very important wherever fertilizers are not used or when the amount spilled is insufficient. It then strongly limits the productivity of the crop and the grain biomass (not shown). Assimilating the realistic crop height throughout the growing season changes the simulated latent and sensible heat fluxes within 10% of their maximum value at the peak of the growing season.

4.2. Evaluation of the simulated evapotranspiration and net CO₂ flux

Testing our model against continuous H_2O and CO_2 flux measurements (made using the eddy covariance method) is crucial to assess its performance in the view of an upcoming coupling with atmospheric models. We selected two sites from the Ameriflux network (Falge et al. 2000) where meteorological and flux data have been measured at the half-hourly time step: a winter wheat field at Ponca, Oklahoma (36°46′N, 97°08′W), and a corn field at Bondville, Illinois (40°00′N, 88°17′W). Sowing occurred on 14 October 1996 at Ponca (day 287; G. George 2001, personal communication), and 1 May 1997 at Bondville (day 121; T. Meyers 2001, personal communication). The harvest date is computed by STICS from the GDD concept used for leaf cycle and grain filling.

Figures 7a–d shows the seasonal evolution of net ecosystem exchange (NEE) and observed ETR, simulated by ORCHIDEE-STICS, and by the standard version of ORCHIDEE, while Figures 8, 9, and 10 show the correlations between the observed and modeled fluxes. ORCHIDEE-STICS reproduces very well the overall timing and amplitude of NEE throughout the year [with a best-fit line that is almost the 1:1 line, and a correlation coefficient of 0.8753 for winter wheat (Figure 8a) and of 0.9571 for corn (Figure 9a)], as well as the short-term variability within the

Table 4. Figure of Merit in Time (FMT), which is a statistical coefficient of the time analysis (see description below), for a number of variables simulated by ORCHIDEE-STICS at the winter wheat site of Grignon. These coefficients are computed to compare the different versions listed in Table 3 (S0 = ORCHIDEE, through S5) to ORCHIDEE-STICS (i.e., S6). The last line only compares ORCHIDEE-STICS to measurements. The FMT evaluates the overlap between two curves, normalized to the maximum value predicted at each time. The FMT is expressed in percent. A temporal shift of the time series can significantly reduce the FMT, even if predicted duration and absolute values are in good agreement. Also, a difference between predicted values can give a small FMT, even if time of arrival and duration are correctly predicted.
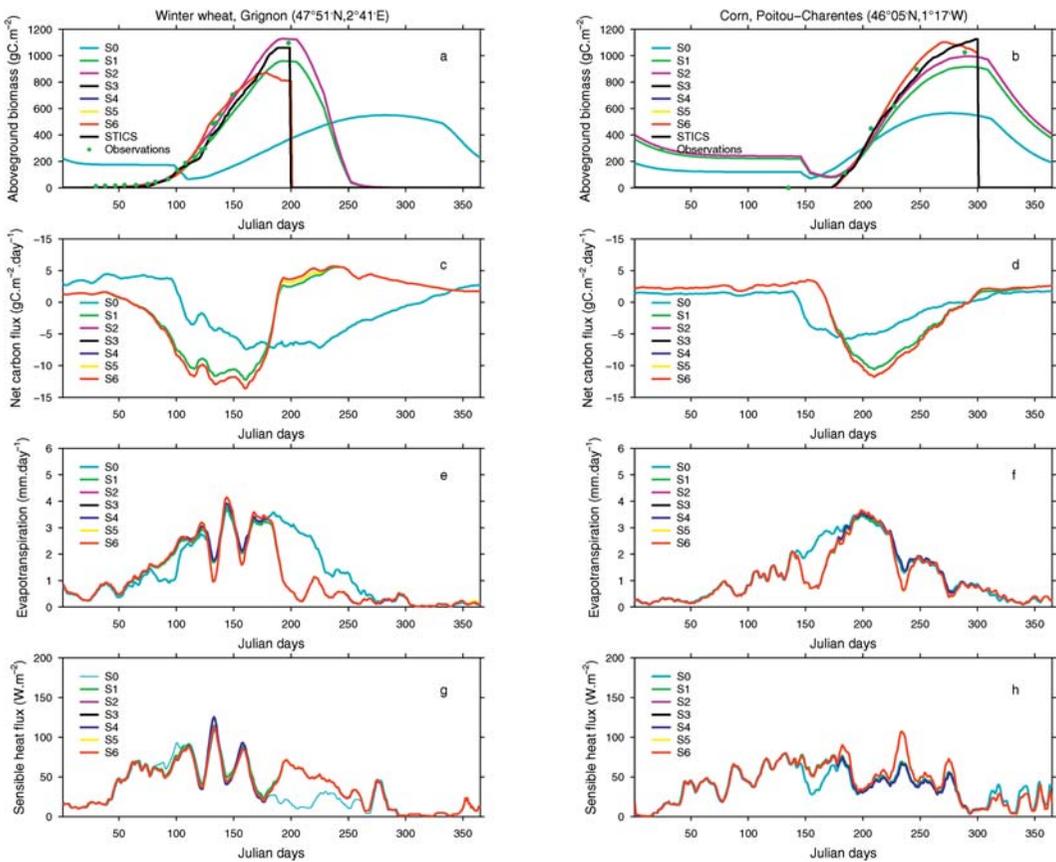
Simulation	Aboveground biomass whole year	Aboveground biomass from emergence through harvest	Evapo-transpiration whole year	Sensible heat flux whole year	Carbon net flux whole year	Soil water content whole year	Water stress index whole year
S0	15.4	37.8	78.6	76.4	12.4	86.4	68.1
S1	52.7	94.1	92.1	91.3	40.4	93.6	83.4
S2	45.8	85.4	96.6	96.1	42.4	95.1	85.5
S3	100	100	96.6	96.1	100	96.6	85.5
S4	100	100	96.6	96.1	100	96.6	97.6
S5	100	100	100	100	100	100	100
S6	100	100	100	100	100	100	100
Model/data	82.3	83.8					

crop season. ORCHIDEE, on the other hand, as already discussed for aboveground biomass, is obviously out of phase for winter wheat (Figure 10a) and the growing season is too long for corn with underestimated peak values (Figure 10e; the best-fit line is quite different from 1:1).

The wheat (corn) field acts as a net sink of atmospheric CO_2 between day 40 (160) and 140 (250), and as a net source the rest of the year. At both sites this change in behavior (w.r.t. CO_2) occurs shortly before harvest (Figures 7e,f) at a

Table 5. Same as Table 4 but at the corn site of Poitou-Charentes.

Simulation	Aboveground biomass whole year	Aboveground biomass from emergence through harvest	Evapo-transpiration whole year	Sensible heat flux whole year	Carbon net flux whole year	Soil water content whole year	Water stress index whole year
S0	71.2	68.4	81.9	85.4	66.8	87.6	75.6
S1	79.7	96.7	91.6	93.3	76.6	97.6	81.6
S2	82.8	100	93.6	93.8	79.3	99.1	82.2
S3	100	100	95.1	93.8	100	99.1	82.2
S4	100	100	95.1	93.8	100	99.1	98.9
S5	100	100	100	100	100	100	100
S6	100	100	100	100	100	100	100
Model/data	55.8	87					

Figure 6. Temporal evolution of observed (green triangles) and simulated (plain lines) variables, starting 1 Jan (Julian day 1) and ending 31 Dec (Julian day 365). Simulated values from STICS are plotted using the black line, results from ORCHIDEE are plotted using the blue line, and those from ORCHIDEE-STICS are plotted using the red line. Other colors are used for different versions of ORCHIDEE-STICS (see Table 3 for the list). Results are shown for (a), (c), (e), (g) winter wheat at Grignon in 1995 and (b), (d), (f), (h) corn in Poitou-Charentes in 1996. (a),(b) Total above ground biomass (sum of leaves, stems, fruits, and reserves in gC m^{-2}); (c),(d) net carbon flux emitted by the land surface (gC m^{-2} day^{-1}; negative values indicate a biospheric sink); (e),(f) total evapotranspiration (mm day^{-1}); and (g),(h) sensible heat flux (W m^{-2}).

time when most leaves are senescent and photosynthesis cannot compensate for respiration. ORCHIDE-STICS reproduces very well the timing from sink to source (and vice versa) for corn (at Bondville), while a delay of about 6 days is obtained for wheat (at Ponca). We have no LAI measurements at Ponca; therefore, we have no means to examine whether this delay could be explained by a similar delay in the simulated leaf cycle in 1997. But the hypothesis of a delayed growth of leaves in our model seems consistent with the growth rate of the net CO_2 sink (i.e., slower in our model than in reality), and correlation with observations is even better after
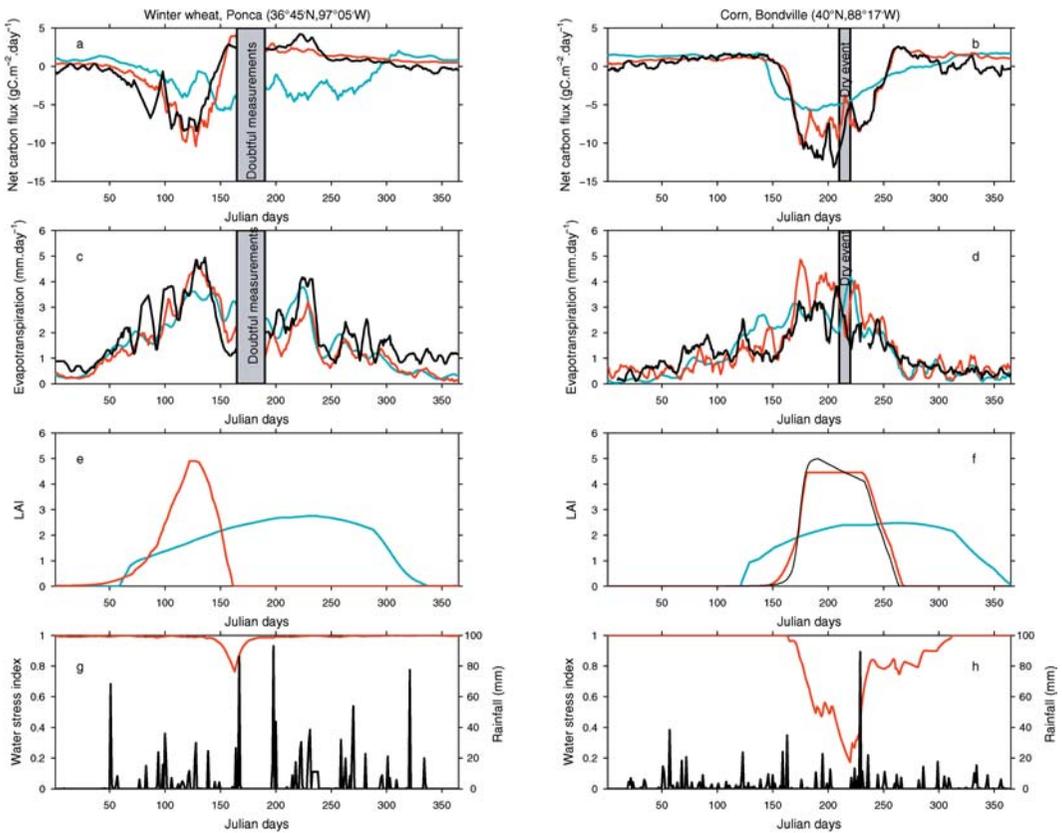
Figure 7. Temporal evolution of a number of observed (plain black line) and simulated (blue line for ORCHIDEE and red line for ORCHIDEE-STICS) variables at the two U.S. sites: (a), (c), (e), (g) winter wheat at Ponca and (b), (d), (f), (h) corn at Bondville. (a),(b) Net ecosystem exchange ($gC\ m^{-2}\ day^{-1}$). Negative values represent a sink of CO_2 with respect to the atmosphere, while positive values represent a source. (c),(d) Total evapotranspiration ($mm\ day^{-1}$); (e),(f) LAI; (g),(h) observed rainfall ($mm\ day^{-1}$; black line) and simulated water stress (red line). All values are presented as 5-day running means to smooth out very high frequencies. The vertical gray bar corresponds to a time period with measurements problems at Ponca, while it highlights the influence of water stress at Bondville.

accounting for the hypothesized delay [the correlation coefficient increases during the growing season (Figures 8b,f) from 0.8112 to 0.86 711 for NEE, and from 0.7065 to 0.8724 for ETR (Figures 8c,d,g,h) when accounting for the shift]. At Bondville (corn) the seasonal evolution of LAI is extremely well reproduced by ORCHIDEE-STICS (Figure 7f).

During the growing season, the observed maximum CO_2 uptake is larger for corn ($\sim-12\ gC\ m^2\ day$) than for wheat ($\sim-8\ gC\ m^{-2}\ day^{-1}$), while in the simulations it is of about the same magnitude ($\sim-10\ gC\ m^{-2}\ day^{-1}$). The slight overestimation of the carbon sink in our model at the peak of the growing season
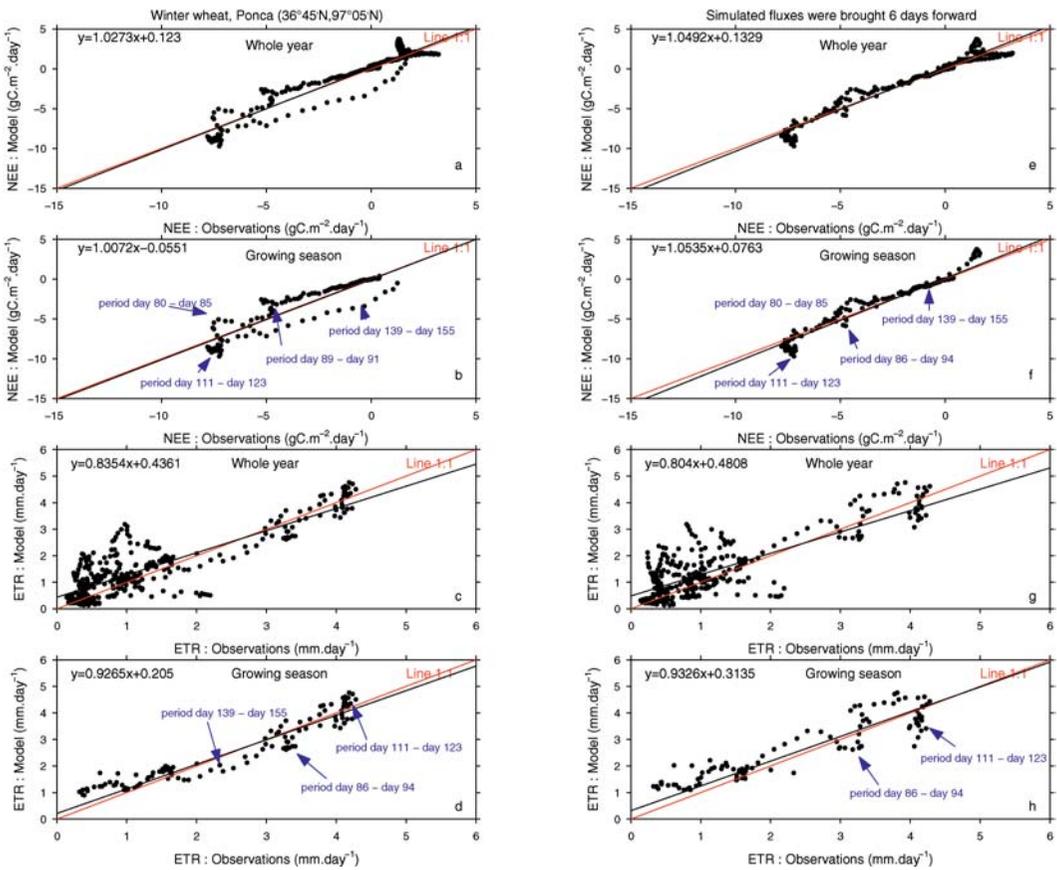
Figure 8. Scatterplots showing the results obtained with ORCHIDEE-STICS vs observations at Ponca (winter wheat) for (a) NEE throughout the year, (b) NEE throughout the crop season (from emergence to harvest, i.e., day 310 of previous year to day 160), (c) ETR throughout the year, and (d) ETR throughout the crop season. The same variables are presented in (e)–(h) but once the model results have been shifted by 6 days to account for the supposed delay in leaf growth. The red line in all plots corresponds to the 1:1 line. Regression coefficients are computed with respect to the black lines (i.e., best fit).

could result from a delay in the growth of leaves, as suggested above, whereas in reality senescence has already started. At the corn site, the strong underestimation of the carbon sink, despite its correct timing, results from the water stress simulated by ORCHIDEE (Figure 7h), which limits photosynthesis and therefore the net uptake CO_2 flux. However, the simulated water stress (due to the lack of precipitation) is not sufficient for STICS to initiate irrigation. In reality corn had not been watered; therefore, the larger observed sink could be due to either the absence of water stress (suggesting an unrealistically high evapotranspiration rate in ORCHIDEE-STICS) or to the crop cultivar selected (the U.S. corn may be more resistant to rainfall deficit, i.e., have a much larger water-use efficiency, thereby lowering water losses while maintaining large rates of photosynthesis).
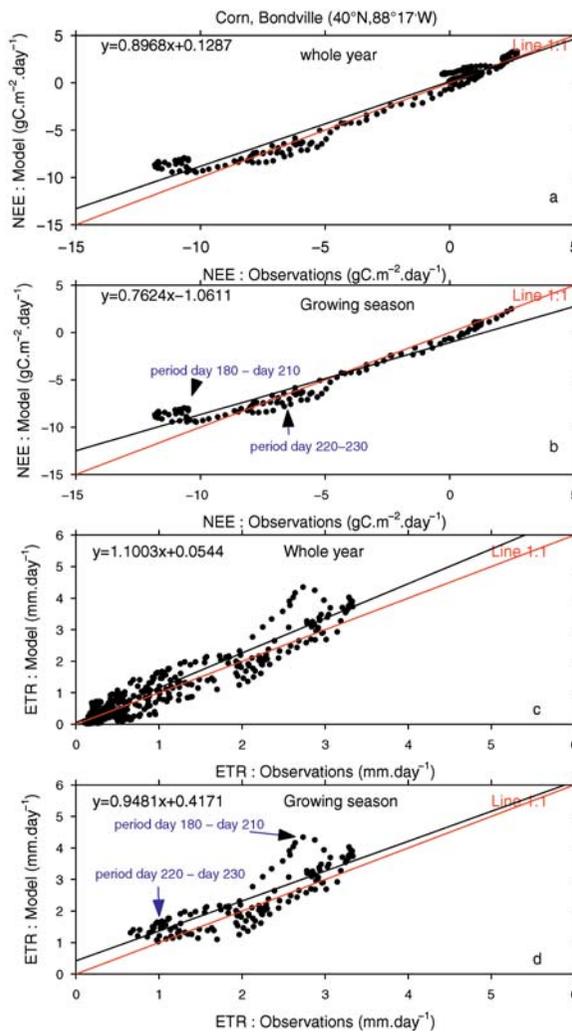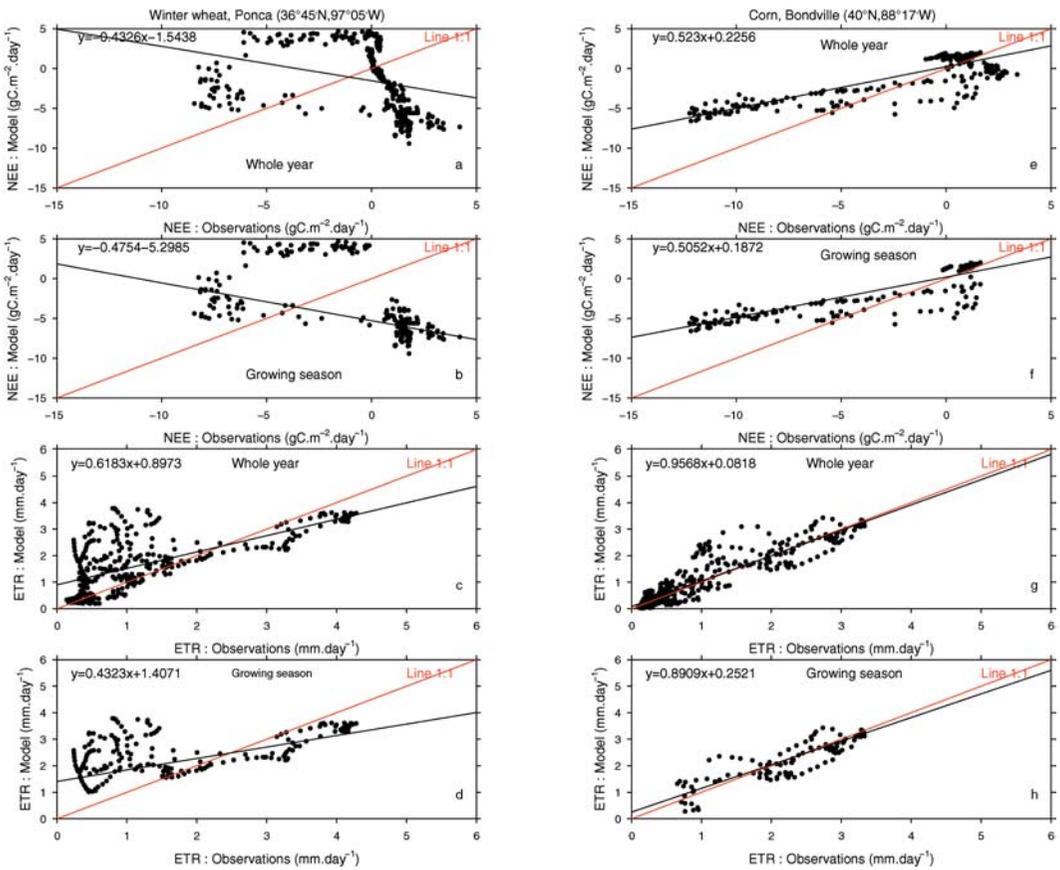
Figure 9. Same as Figure 8 except at Bondville (corn) for (a) NEE throughout the year, (b) NEE throughout the crop season (from emergence to harvest, i.e., day 133 to day 260), (c) ETR throughout the year, and (d) ETR throughout the crop season.

At harvest (i.e., day 160 for winter wheat and day 260 for corn in the model) there is an observed peak of CO_2 release to the atmosphere (of about 3–4 gC m^{-2} day^{-1}), which is well reproduced by the model at both sites. Litter is then added to the soil and starts to decompose. However, the simulated rate of decomposition is much lower than the one observed at Bondville (corn). Ploughing is not included in ORCHIDEE-STICS, while in reality it occurred shortly after harvest and helped accelerate litter decomposition. Moreover, because the net outgoing CO_2 flux is lower (or equal) during the whole year in reality, our assumption is that less material is left on the ground by farmers, while in ORCHIDEE-STICS all leaves and stems become litter. At Ponca (winter wheat), the simulated rate of decomposition is of the right order of magnitude, except for the peak observed

Figure 10. Same as Figure 8 except the results obtained with the standard version of ORCHIDEE vs observations (a)–(d) at Ponca (winter wheat) and (e)–(g) at Bondville (corn) for (a),(e) NEE throughout the year; (b),(f) NEE throughout the crop season (from observed emergence to harvest); (c),(g) ETR throughout the year; and (d),(h) ETR throughout the crop season.

from days 200 to 220, which is related to ploughing (not included in ORCHIDEE-STICS).

There are substantial observed short-term fluctuations (episodes of 10–20-day duration) in NEE and ETR at both sites, especially during the growing season, that are rather well reproduced by ORCHIDEE-STICS. At Bondville (corn), for example, observed NEE suddenly increases (reduced CO_2 sink) between days 220 and 230 and is associated with a sharp decrease in ETR (Figure 7d, vertical gray lines). The same rapid changes also occur in the model, with similar amplitude, but about 10 days earlier than observed. In both cases (model and data), rain deficit is responsible (no rain was observed between days 205 and 220; Figure 7h), but the water stress response it induces seems to occur more slowly in reality than in the model, which responds to drought with almost no time lag. ORCHIDEE-STICS was already experiencing some water stress prior to this rain deficit and therefore reacted instantaneously to this new dry event. We believe that, in reality, soil

moisture was still abundant prior to this event, and the stress was therefore only felt when evapotranspiration had extracted enough water from the soil.

Sharp changes in NEE and ETR are also observed and modeled at Ponca (winter wheat) at the beginning of the growing season (~day 90; Figures 7a,c vertical dotted line). However, the simulated amplitude is smaller because LAI is still very low in ORCHIDEE, whereas it is probably larger in reality (given the large absolute NEE values observed). Moreover, and unlike what is observed at the corn site, the timing of this fluctuation is the same in the model as in reality. At the beginning of the growing season the soil is still wet enough for a rain deficit to be of less consequence (Figure 7g).

Outside of the growing season the simulated ETR is generally smaller than observed. If any natural grass is allowed to grow before crop sowing, then the discrepancy between model and data is understandable since bare ground is prescribed to ORCHIDEE-STICS after harvest. However, we have no field data to confirm this hypothesis, and therefore no means to check the quality of our simulation during that time period.

5. Concluding remarks

Cultivated plants are selected and grown to produce optimum yield and, as a result, might be less sensitive to, or more protected against, external factors (e.g., water stress, cold temperatures, and high wind) than wild species are. The impacts of spatially varying climate can therefore be exploited or counteracted by agricultural practices (e.g., choice of species and cultivars, irrigation, and fertilization) resulting in less spatially variable surface–atmosphere exchanges (e.g., latent and sensible heat flux, CO_2 flux). It is therefore crucial to account for these practices in land surface models for a more accurate simulation of carbon–water–energy fluxes, and of carbon and water stocks.

In this paper we focused on the two major cereal species found in European temperate regions (i.e., corn and winter wheat) and adapted our "generic" global terrestrial biosphere model (ORCHIDEE) in order to improve its representation of these ecosystems. To achieve this goal, we used the crop model STICS to produce "data" (with respect to, e.g., leaf and root area index, nitrogen stress, and vegetation height), and modified some formulations (e.g., allocation and water stress) and parameters (e.g., rates of carboxylation and RuBP regeneration) in ORCHIDEE to allow these external data to be assimilated in a proper way.

A similar approach has been adopted by Olioso et al. (Olioso et al. 2001; Olioso et al. 2002) using STICS to assimilate remotely sensed variables into another soil–vegetation–atmosphere transfer scheme. Kucharik and Brye (Kucharik and Brye 2003), on the other hand, have chosen to include adequate and mechanistic parameterizations of crop phenology in their dynamic global vegetation model to examine the simultaneous response of nitrate nitrogen leaching losses and maize yield to different amounts of nitrogen fertilizer. Both approaches are quite different but, if applied at the global scale, will meet the exact same problem, that is, the availability of a global description of crop distribution and management options (e.g., irrigation, fertilizer application, planting date, tillage). Our method has the advantage of using a *generic* crop model that has been thoroughly *validated* at

many different sites, using many different cultivars, and is *still under development* and *improvement* in many different agronomic research laboratories.

ORCHIDEE-STICS has been evaluated at four different sites. The simulated aboveground biomass, net ecosystem exchange, and evapotranspiration are in good agreement with observations (both amplitude and timing) despite the lack of data on agricultural practices. This increases our confidence in the future use of this model at the regional and global scale. Its improvements described here should improve our simulation of present-day climate and climate variability. Moreover, with respect to future climate change scenarios, our "coupled" model will allow us not only to simulate changes in agricultural yield in response to climate change, but also to simultaneously account for feedbacks between changes in crop behavior and the atmospheric state and circulation.

References

Alcamo, J., and Coauthors,1998: Global modelling of environmental change: An overview of IMAGE 2.1. *Global Change Scenarios of the 21st Century: Results from the IMAGE 2.1 Model*. J. Alcamo, R. Leemans, and E. Kreileman, Eds., Elsevier Science, 3–94.

Arrouyas, D., J. Balesdent, J.C. Germon, P.A. Jayet, J.F. Soussana, and P. Stengel, 2002: Contribution à la lutte contre l'effet de serre. Stocker du carbone dans les sols agricoles de France? Expertise scientifique collective INRA, 332 pp.

Boote, K.J., J.W. Jones, and N.B. Pickering, 1996: Potential uses and limitations of crop models. *Agron. J.,* **88,** 704–716.

Botta, A., N. Viovy, P. Ciais, P. Friedlingstein, and P. Monfray, 2000: A global prognostic scheme of leaf onset using satellite data. *Global Change Biol.,* **15,** 709–725.

Betts, R.A., 1999: The impact of land-use on the climate of present day. Research activities in atmospheric and oceanic modeling, CAS/JSCE WGNE Rep. 28, WMO, Geneva, Switzerland, 7.11–7.12.

Brisson, N., and Coauthors, 1998: STICS: A generic model for the simulation of crops and their water and nitrogen balances. I. Theory and parameterisation applied to wheat and maize. *Agronomie,* **18,** 311–346.

——, and Coauthors, 2002a: An overview of the crop model STICS. *Eur. J. Agron.,* **18,** 309–332.

——, and Coauthors, 2002b: STICS: A generic model for the simulation of crops and their water and nitrogen balance. II. Model validation for wheat and maize. *Agronomie,* **22,** 69–93.

Choisnel, E., 1977: Le bilan d'énergie et le bilan hydrique du sol. *La Météorologie,* **6** (11), 103–133.

Collatz, G.J., M. Ribas-Carbo, and J.A. Berry, 1992: Coupled photosynthesis-stomatal conductance model for leaves of C_4 plants. *Aust. J. Plant. Physiol.,* **19,** 519–538.

Cox, P. M., R. A. Betts, C. D. Jones, S. A. Spall, and I. J. Totterdell, 2000: Acceleration of

global warming due to carbon-cycle feedbacks in a coupled climate model. *Nature,* **408,** 184–197.

de Noblet-Ducoudré, N., S. Gervois, P. Ciais, N. Viovy, N. Brisson, B. Seguin, and A. Perrier, 2005: Coupling the Soil–Vegetation Atmosphere Transfer Scheme ORCHIDEE to the agronomy model STICS to study the influence of croplands on the European carbon and water budgets. *Agronomie,* in press.

de Rosnay, P., and J. Polcher, 1998: Modeling root water uptake in a complex land surface scheme coupled to a GCM. *Hydrol. Earth Syst. Sci.,* **2,** 239–255.

de Wit, C.T., 1978: Simulation of assimilation respiration and transpiration of crops. *Simulation Monogr.,* Pudoc, 141 pp.

Ducoudré, N., K. Laval, and A. Perrier, 1993: SECHIBA, a new set of parameterizations of the hydrologic exchanges at the land–atmosphere interfaces within the LMD atmospheric general circulation model. *J. Climate,* **6,** 248–273.

Dufresne, J.-L., L. Fairhead, H. LeTreut, L. Berthelot, L. Bopp, P. Ciais, P. Friedlingstein, and P. Monfray, 2002: On the magnitude of positive feedback between future climate change and the carbon cycle. *Geophys. Res. Lett.,* **29,** 1405, doi:10.1029/2001GL013777.

du Monceau, D., 1761: Traité de la culture des terres, suivant les principes de M. Tull. Anglais 6 tomes, Paris.

Falge, E., and Coauthors, 2000: Gap filling strategies for defensible annual sums of net ecosystem exchange. *Agric. For. Meteor.,* **170,** 71–77.

Farquhar, G.D., S. von Caemmerer, and J.-A. Berry, 1980: A biochemical model of photosynthetic CO_2 assimilation in leaves of C_3 species. *Planta,* **149,** 78–90.

Friedlingstein, P., G. Joel, C.B. Field, and Y. Fung, 1998: Toward an allocation scheme for global-terrestrial carbon models. *Global Change Biol.,* **5,** 755–770.

——, J.-L. Dufresne, P.M. Cox, and P. Rayner, 2003: How positive is the feedback between climate change and the carbon cycle? *Tellus,* **55B,** 692–700.

Gregory, P.J., J.A. Palta, and G.R. Batts, 1997: Root systems and root mass ratio—Carbon allocation under current and projected atmospheric conditions in arable crops. *Plant Soil,* **187,** 221–228.

Hansen, S., H.E. Jensen, N.E. Nielsen, and H. Swenden, 1990: DAISY, a soil-plant system model. Danish simulation model for transformation and transport of energy and matter in the soil plant atmosphere system, National Agency for Environmental Protection, Copenhagen, Denmark, 369 pp.

Janssens, I.A., and Coauthors, 2003: Europe's terrestrial biosphere absorbs 7% to 12% of European anthropogenic CO_2 emissions. *Science,* **300,** 1538–1542.

Jones, C.A., J.T. Ritchie, J.R. Kiniry, and D.C. Goodwin, 1986: Subroutine structure. *CERES Maite: A Simulation Model of Maite Growth and Development,* C.A. Jones and J.R. Kiniry, Eds., Texas A&M Press, 49–105.

Krinner, G., and Coauthors, 2005: A dynamical global vegetation model for studies of the coupled atmosphere–biosphere system. *Global Biogeochem. Cycles,* in press.

Kucharik, C.J., 2003: Evaluation of a process-based agro-ecosystem model (Agro-IBIS) across the U.S. Corn Belt: Simulations of interannual varaibility in maize yield. *Earth Interactions,* 7. [Available online at http://EarthInteractions.org.]

——, and K.R. Brye, 2003: Integrated BIosphere Simulator (IBIS) yield and nitrate loss predictions for Wisconsin maize receiving varied amounts of nitrogen fertilizer. *J. Environ. Qual.,* **32,** 247–267.

Nobre, C., P.J. Sellers, and J. Shukla, 1991: Amazonian deforestation and regional climate change. *J. Climate,* **4,** 957–988.

Olioso, A., Y. Inoue, J.P. Wigneron, O.Ortega-Farias, P. Lecharpentier, M. Pardé, J.C. Calvet,

and O. Inizan, 2001: Using a coupled crop-SVAT model to assess crop canopy processes from remote sensing data. *IGARSS 2001*, Sydney, Australia, IEEE Publications.

——, and Coauthors, 2002: Assimilation of remote sensing data into crop simulation models and SVAT models. *First Int. Symp. on Recent Advances in Quantitative Remote Sensing*, Valencia, Spain, Publicacions de la Universitad de València, 329–338.

Polcher, J., K. Laval, L. Dümenil, J. Lean, and P.R. Rowntree, 1996: Comparing three land surface schemes used in GCMs. *J. Hydrol.,* **18,** 373–394.

Ritchie, J.T., and S. Omer, 1984: Description and performance of CERES-Wheat, a user-oriented wheat yield model. USDA-ARS-SR Grassland Soil and Water Research Laboratory, Temple, TX, 159–175.

Sitch, S., and Coauthors, 2003: Evaluation of ecosystems dynamics, plant geography and terrestrial carbon cycling in the LPJ dynamic global vegetation model. *Global Change Biol.,* **9,** 161–185.

Smith, P., R. Milne, D.S. Powlson, J.U. Smith, P.D. Falloon, and K. Coleman, 2000: Revised estimates of the carbon mitigation potential of UK agricultural land. *Soil Use Manage.,* **16,** 293–295.

van Deipen, C.A., J. Wolf, H. van Keulen, and C. Rappoldt, 1989: WOFOST: A simulation model of crop production. *Soil Use Manage.,* **5,** 16–24.

Vitousek, P. M., H. A. Mooney, J. Lubchenco, and J.M. Melillo, 1997: Human domination of Earth's ecosystems. *Science,* **277,** 494–499.

Vleeshouwers, L.M., and A. Verhagen, 2002: Carbon emission and sequestration by agricultural land use: A model study for Europe. *Global Change Biol.,* **8,** 519–530.

Williams, J.R., C.A. Jones, and P.T. Dyke, 1984: A modeling approach to determining the relationship between erosion and soil productivity. *Trans. ASAE,* **27,** 129–144.

Wullschleger, S.D., 1993: Biochemical limitations to carbon assimilation in C_3 plants, A retrospective analysis of the A/Ci curves from 109 species. *J. Exp. Bot.,* **44,** 907–920.

Xue, Y., and J. Shukla, 1993: The influence and land surface properties on Sahel climate. Part I: Deforestation. *J. Climate,* **6,** 2232–2246.

Zhao, M., A.J. Pitman, and T. Chase, 2001: The impact of land cover change on the atmospheric circulation. *Climate Dyn.,* **17,** 467–477.